This article has been accepted for publication in a future issue of this journal, but has not been fully edited. Content may change prior to final publication. Citation information: DOI 10.1109/JBHI.2016.2582340, IEEE Journal of Biomedical and Health Informatics

ECG Denoising Using Marginalized Particle Extended Kalman Filter with an Automatic Particle Weighting Strategy

Hamed Danandeh Hesar and Maryam Mohebbi

***Abstract*— In this paper a model-based Bayesian filtering framework called the "marginalized particle-extended Kalman filter (MP-EKF) algorithm" is proposed for electrocardiogram (ECG) denoising. This algorithm does not have the extended Kalman filter (EKF) shortcoming in handling non-Gaussian non-stationary situations because of its nonlinear framework. In addition, it has less computational complexity compared with particle filter. This filter improves ECG denoising performance by implementing marginalized particle filter framework while reducing its computational complexity using EKF framework. An automatic particle weighting strategy is also proposed here that controls the reliance of our framework to the acquired measurements. We evaluated the proposed filter on several normal ECGs selected from MIT-BIH normal sinus rhythm database. To do so, artificial white Gaussian and colored noises as well as non-stationary real muscle artifact (MA) noise over a range of low SNRs from 10 to -5 dB were added to these normal ECG segments. The benchmark methods were the EKF and extended Kalman smoother (EKS) algorithms which are the first model-based Bayesian algorithms introduced in the field of ECG denoising. From SNR viewpoint, the experiments showed that in the presence of Gaussian white noise, the proposed framework outperforms the EKF and EKS algorithms in lower input SNRs where the measurements and state model are not reliable. Owing to its nonlinear framework and particle weighting strategy, the proposed algorithm attained better results at all input SNRs in non-Gaussian non-stationary situations (such as presence of pink noise, brown noise, and real muscle artifacts). In addition, the impact of the proposed filtering method on the distortion of diagnostic features of the ECG was investigated and compared with EKF/EKS methods using an ECG diagnostic distortion measure called the "Multi-Scale Entropy Based Weighted Distortion Measure" or MSEWPRD. The results revealed that our proposed algorithm had the lowest MSEPWRD for all noise types at low input SNRs. Therefore, the morphology and diagnostic information of ECG signals were much better conserved compared with EKF/EKS frameworks, especially in non-Gaussian non-stationary situations.**

***Index Terms*— ECG denoising, extended Kalman filtering, model-based filtering, nonlinear Bayesian filtering, Rao-blackwellized particle filtering.**

H. Danandeh Hesar is with the Department of Biomedical Engineering, K. N. Toosi University of Technology, Tehran, Iran (e-mail: h_danandeh@ee.kntu.ac.ir).

M. Mohebbi is with the Department of Biomedical Engineering, K. N. Toosi University of Technology, Tehran, Iran (e-mail: m.mohebbi@kntu.ac.ir).

I. Introduction

Electrocardiogram (ECG) is widely popular among physicians because it contains helpful information for cardiac disease analysis and diagnosis. Due to presence of environmental and non-environmental interferences during ECG recording such as electromyographic (EMG) noise, noise originating from electrode misplacement, etc, ECG denoising remains a major concern for researchers. Non-model-based methods including *Principal Component Analysis* (PCA) [1], *Independent Component Analysis* (ICA) [2], [3], *Neural Networks* (NNs) [4], *Wavelet Denoising* (WD) [5]-[7], *Ensemble Averaging* (EA) [8] and *Adaptive Filtering* (AF) [9], [10] have been widely used to remove ECG contaminants.

Some other researchers proposed to use model-based methods for ECG processing. McSharry *et al.* proposed a three state nonlinear dynamical model in Cartesian space for ECG synthesis [11]. Many researchers used the ECG Dynamical Model (EDM) proposed by McSharry *et al.* and Bayesian filtering approach, to solve the problem of ECG denoising and feature extraction. In [12], Sameni *et al.* converted the EDM to a simplified 2-state polar EDM in order to implement an extended Kalman filter (EKF) based algorithm (also known as EKF2) for denoising ECG signals. Sayadi *et al.* extended Sameni's model by adding the characteristic parameters of polar EDM to state model and considered them as Auto Regressive (AR) states [13], [14]. Sayadi *et al.* used this modified model for ECG denoising and fiducial points extraction and stated that it exhibits better results compared with its predecessor [13], [14]. Also, in [15], the polar EDM was modified to represent a Gaussian wave-based state space model in which some states characterized certain segments of ECG wave, i.e. P, QRS, and T.

In some works, the effects of applying particle filter (PF) for ECG signal processing were studied. Readers may refer to [16] for more information about particle filters. Lee *et al.* in [17] used a particle filter based framework along with a modified polar EDM in order to extract the atrial signal from ECG for detection of Atrial Flutter (AFL) and Atrial Tachycardia (AT). To overcome the computational complexity of PF, Lin *et al.* in [18] proposed to use a marginalized particle filter (MPF) for ECG denoising and implemented the "triangular" model proposed by Schön *et al.* [19]. However using the "triangular" model, not only required a notable modification of the original 2-state polar

This article has been accepted for publication in a future issue of this journal, but has not been fully edited. Content may change prior to final publication. Citation information: DOI 10.1109/JBHI.2016.2582340, IEEE Journal of Biomedical and Health Informatics

EDM, but also limited the choices of linear states. In other words, in this algorithm, some linear AR states had to be approximated using PF that would increase computational complexity.

The nonlinear nature of ECG signal itself and the presence of non-Gaussian non-stationary noises such as muscle artifact (MA) noise restrain EKF-based frameworks to reach an optimal recursive solution. Moreover, in highly noise contaminated ECGs, the state model or the measurements are not reliable. These limitations motivate us to look for better solutions using other Bayesian based frameworks such as particle filters. However, we intend to benefit from both EKF and particle filter frameworks. In other words, we want to improve ECG denoising performance by implementing PF framework while reducing its computational complexity using EKF framework. To do so, in this paper, a new Bayesian filtering framework is introduced which utilizes both marginalized particle filter and EKF frameworks. With minimal modification in the 2-state polar EDM [12] (adding a third state), the proposed framework can denoise highly noise contaminated ECG signals more efficiently. We also propose an automatic particle weighting strategy that balances the dependency of the framework to the obtained measurements. This strategy effectively aids the algorithm in estimation of the ECG signals at low input SNRs. The benchmark methods to evaluate our algorithm are the EKF and extended Kalman smoother (EKS) denoising algorithms which were first introduced in [12]. From SNR viewpoint, the experiments show that in the presence of Gaussian white noise, the proposed framework outperforms the other two algorithms at lower input SNRs. The simulations also indicate that it attains better results in non-Gaussian situations such as presence of pink noise, brown noise, and real muscle artifacts at all input SNRs. Another advantage of this framework is its implementing flexibility with other variants of EDM. In addition, the impact of the proposed filtering method on the distortion of diagnostic features of the ECG was studied and compared with EKF/EKS methods for 4 different noise types at 4 low input SNRs. The results proved that the morphology and diagnostic information of ECG signals are much better conserved in comparison to the EKF/EKS frameworks.

This paper is organized as follows. Section 2 provides an introduction to EDM and marginalized particle filter concept. The proposed algorithm is presented in Section 3. The experimental results and analyses are given in Section 4 and finally conclusions are drawn in the last Section.

II. ECG Dynamical Model and Rao-Blackwellized Particle Filter

In this section, the EDM and its variants for EKF based denoising frameworks are explained briefly. Then the marginalized particle filter concept is reviewed.

A. ECG Dynamical Model and Extended Kalman Filter

McSharry *et al.* in [11] proposed a three dimensional state differential equation for ECG synthesis in Cartesian space. The model characterizes the ECG as summation of 5 Gaussian kernels corresponding to ECG feature segments i.e. P, Q, R, S and T waves. This model is as follows:

$$\begin{aligned} x' &= \alpha x - \omega y \\ y' &= \alpha y + \omega x \\ z' &= -\sum_{j\in\{P,Q,R,S,T\}} a_j \Delta\theta_j \exp\left(-\frac{\Delta\theta_j^2}{2b_j^2}\right) - (z - z_0). \end{aligned} \tag{1}$$

In the above model $x' = \frac{dx}{dt}$ (derivation of x with respect to time), the same goes for y' and z', $z = 1 - \sqrt{x^2 + y^2}$, $\Delta\theta_j = (\theta - \theta_j) \bmod (2\pi)$, $\theta = \tan^{-1}\left(\frac{y}{x}\right)$, $\omega = \frac{2\pi}{T}$ (T is RR peak interval in time). a_j, b_j, θ_j $(j \in P, Q, R, S, T)$ are the amplitude, angular width, and location of each Gaussian kernel, respectively. By changing these feature parameters, one can synthesize many types of ECG signals on a circle with radius $r = 1$ and phase between 0 and 2π (or $-\pi$ and π). In addition, Mcsharry *et al.* added the parameter z_0 in order to model the baseline wander in the synthetic phase wrapped ECG.

In [12], Sameni *et al.* converted this model to a compact discrete time state space polar form. This model had only two states as follows:

$$\begin{cases} \varphi_{k+1} = (\varphi_k + \omega\delta) \bmod (2\pi) \\ z_{k+1} = -\sum_{j\in\{P,Q,R,S,T\}} \omega\delta \frac{a_j \Delta\theta_j}{b_j^2} \exp\left(-\frac{\Delta\theta_j^2}{2b_j^2}\right) + z_k + \eta \end{cases} \tag{2}$$

where δ is the sampling period, $\Delta\theta_j = (\varphi_k - \theta_j) \bmod (2\pi)$ and η is a random Gaussian white noise which models the uncertainty of the modified EDM. Other variables are similar to the namesake variables in (1). Sameni *et al.* used this model to construct an EKF based denoising framework and called it "EKF2" [12]. Sayadi *et al.* added the 15 feature parameters a_j, b_j, θ_j as AR states to the aforementioned polar model and used the same EKF based approach to denoise and compress ECG signals [13] and proposed a method to extract the fiducial points in each ECG cycle [14]. They also proposed a Gaussian wave-based state space model in which some states correspond to certain segments of ECG wave, i.e. P, QRS and T. This 4-state model was used for premature ventricular contractions (PVC) identification [15].

B. Marginalized Particle Filter

The basic idea in marginalized particle filter is to decrease the variances of state estimates by separating the linear states from nonlinear states in mixed linear/nonlinear state space models. This method is sometimes called Rao-Blackwellization [20]. In marginalized particle filter, it is assumed that the state vector $\mathbf{x}_k$ consists of a linear state vector $\mathbf{x}_k^L$ and a nonlinear state vector $\mathbf{x}_k^{NL}$, i.e. $\mathbf{x}_k = \begin{bmatrix} \mathbf{x}_k^L \\ \mathbf{x}_k^{NL} \end{bmatrix}$. The linear states are estimated using

This article has been accepted for publication in a future issue of this journal, but has not been fully edited. Content may change prior to final publication. Citation information: DOI 10.1109/JBHI.2016.2582340, IEEE Journal of Biomedical and Health Informatics

Kalman filter and the nonlinear states are estimated by standard particle filter. In [19], Schön *et al.* introduced three types of models, "diagonal model", "triangular model", and "general model". These models are commonly used in mixed linear/nonlinear state estimation situations. The "general model" describes the state space model in the following way:

$$\mathbf{x}_{k+1}^{NL} = f_k^{NL}\left(\mathbf{x}_k^{NL}\right) + A_k^{NL}\mathbf{x}_k^{L} + G_k^{NL}\boldsymbol{\omega}_k^{NL} \tag{3.a}$$

$$\mathbf{x}_{k+1}^{L} = f_k^{L}\left(\mathbf{x}_k^{NL}\right) + A_k^{L}\mathbf{x}_k^{L} + G_k^{L}\boldsymbol{\omega}_k^{L} \tag{3.b}$$

$$\mathbf{y}_k = h_k^{NL}\left(\mathbf{x}_k^{NL}\right) + C_k^{NL}\mathbf{x}_k^{L} + \mathbf{e}_k . \tag{3.c}$$

In this model, f_k^{NL} and f_k^{L} are nonlinear transition functions of $\mathbf{x}_k^{NL}$. A_k^{NL} and A_k^{L} are transition matrices which are conditionally linear with respect to $\mathbf{x}_k^{NL}$. h_k^{NL} is a nonlinear measurement function of $\mathbf{x}_k^{NL}$ and C_k^{NL} is the measurement matrix that is conditionally linear with respect to $\mathbf{x}_k^{NL}$. The uncertainty is modeled by noise vector $G_k\boldsymbol{\omega}_k = \begin{bmatrix} G_k^{NL}\boldsymbol{\omega}_k^{NL} \\ G_k^{L}\boldsymbol{\omega}_k^{L} \end{bmatrix} \sim N\left(0, Q_k\right)$ in which $Q_k = \begin{bmatrix} Q_k^{NL} & Q_k^{NL,L} \\ (Q_k^{NL,L})^T & Q_k^{L} \end{bmatrix}$ is the state noise covariance matrix and $Q_k^{(NL,L)} = E\{\boldsymbol{\omega}_k^{NL}(\boldsymbol{\omega}_k^{L})^T\}$. The measurement noise is also modeled by $\mathbf{e}_k \sim N\left(0, R_k\right)$ [19].

The "triangular model" is a special case of the "general model" where $G_k^{L} = G_k^{NL} = I$, $E\{\boldsymbol{\omega}_k^{NL}(\boldsymbol{\omega}_k^{L})^T\} = 0$ and $f_k^{L} = 0$, i.e. :

$$\mathbf{x}_{k+1}^{NL} = f_k^{NL}\left(\mathbf{x}_k^{NL}\right) + A_k^{NL}\mathbf{x}_k^{L} + \boldsymbol{\omega}_k^{NL} \tag{4.a}$$

$$\mathbf{x}_{k+1}^{L} = A_k^{L}\mathbf{x}_k^{L} + \boldsymbol{\omega}_k^{L} \tag{4.b}$$

$$\mathbf{y}_k = h_k^{NL}\left(\mathbf{x}_k^{NL}\right) + C_k^{NL}\mathbf{x}_k^{L} + \mathbf{e}_k . \tag{4.c}$$

If (4.a) is rewritten in the following form:

$$\boldsymbol{\xi}_k = \mathbf{x}_{k+1}^{NL} - f_k^{NL}\left(\mathbf{x}_k^{NL}\right) = A_k^{NL}\mathbf{x}_k^{L} + \boldsymbol{\omega}_k^{NL} . \tag{5}$$

It can be deduced that although $\boldsymbol{\xi}_k$ is not an actual measurement of $\mathbf{x}_k^{L}$, it has an additional implicit information about $\mathbf{x}_k^{L}$. The equations (4.c) and (5) are uncorrelated and can be assumed as separate measurements. Based on this idea, the marginalized particle filter for "triangular model" has an additional second prediction step. The marginalized particle filter for "triangular model" is expressed in the following steps [19]:

Step 1: For time-step $k = 0$, with importance distribution $p_{\mathbf{x}_{0|0}^{NL}}\left(\mathbf{x}_{0|0}^{NL}\right)$ and initialization mean $\overline{\mathbf{x}}_0$ and covariance matrix $\overline{P}_0$, initialize the particles $\mathbf{x}_{k|k}^{(i)} = \begin{bmatrix} \mathbf{x}_{k|k}^{NL,(i)} \\ \mathbf{x}_{k|k}^{L,(i)} \end{bmatrix}$ for $i = 1, \ldots, N$ where $\mathbf{x}_{k|k}^{NL,(i)} \sim p_{\mathbf{x}_{0|0}^{NL}}\left(\mathbf{x}_{0|0}^{NL}\right)$ and $\mathbf{x}_{k|k}^{L,(i)} \sim N\left(\overline{\mathbf{x}}_0, \overline{P}_0\right)$.

Step 2: calculate the importance weights for $i = 1, \ldots, N$ using $w_k^{(i)} = p(\mathbf{y}_k | X_k^{NL,(i)}, Y_{k-1})$ where $X_k^{NL,(i)} = \{\mathbf{x}_{0|0}^{NL,(i)}, \mathbf{x}_{1|1}^{NL,(i)}, \ldots, \mathbf{x}_{k|k}^{NL,(i)}\}$, $\mathbf{x}_{k|k}^{NL,(i)}$ is the ith estimated particle of $\mathbf{x}_k^{NL}$ in time-step k and $Y_{k-1} = \{\mathbf{y}_0, \mathbf{y}_1, \ldots, \mathbf{y}_{k-1}\}$. $\mathbf{x}_{k|k}^{NL}$ is the nonlinear estimation of $\mathbf{x}_k^{NL}$ and it is a weighted summation of particles $\mathbf{x}_{k|k}^{NL,(i)}$ $i = 1, \ldots, N$, i.e.:

$$\mathbf{x}_{k|k}^{NL} = \sum_{i=1}^{N} w_k^{(i)}\mathbf{x}_{k|k}^{NL,(i)} . \tag{6}$$

Step 3: normalize importance weights:

$$\tilde{w}_k^{(i)} = \frac{w_k^{(i)}}{\sum_{j=1}^{N} w_k^{(j)}}$$

Step 4: Resample particles if necessary.

Step 5: For each particle $i = 1, \ldots, N$, perform Kalman filter measurement update according to:

$$\hat{\mathbf{x}}_{k|k}^{L,(i)} = \hat{\mathbf{x}}_{k|k-1}^{L,(i)} + K_k\left(\mathbf{y}_k - h_k^{NL}\left(\mathbf{x}_{k|k}^{NL}\right) - C_k\hat{\mathbf{x}}_{k|k-1}^{L,(i)}\right) \tag{7.a}$$

$$P_{k|k}^{(i)} = P_{k|k-1}^{(i)} - K_k C_k P_{k|k-1}^{(i)} \tag{7.b}$$

$$S_k = C_k P_{k|k-1}^{(i)} C_k^T + R_k \tag{7.c}$$

$$K_k = P_{k|k-1}^{(i)} C_k^T S_k^{-1} \tag{7.d}$$

where $\hat{\mathbf{x}}_{k|k}^{L,(i)}$ and $P_{k|k-1}^{(i)}$ are the predicted mean vector and covariance matrix for the linear part of particle $\mathbf{x}_k^{(i)}$ at time-step k, respectively.

Step 6: predict new particles for time-step $k+1$ using importance distribution according to:

$$\mathbf{x}_{k+1|k}^{NL,(i)} \sim p\left(\mathbf{x}_{k+1|k}^{NL} \mid X_k^{NL,(i)}, Y_k\right) \tag{8}$$

Step 7: For each particle $i = 1, \ldots, N$, perform Kalman filter prediction using:

$$\hat{\mathbf{x}}_{k+1|k}^{L,(i)} = A_k^{L}\hat{\mathbf{x}}_{k|k}^{L,(i)} \tag{9.a}$$

$$P_{k+1|k}^{(i)} = A_k^{L} P_{k|k}^{(i)} (A_k^{L})^T + Q_k^{L} \tag{9.b}$$

where $\hat{\mathbf{x}}_{k|k}^{L,(i)}$ and $P_{k|k}^{(i)}$ are the estimated mean vector and covariance matrix for the linear part of particle $\mathbf{x}_k^{(i)}$ at time-step k, respectively.

Step 8: For each particle $i = 1, \ldots, N$, perform second Kalman filter prediction using:

$$\boldsymbol{\xi}_k = \mathbf{x}_{k+1|k}^{NL,(i)} - f_k^{NL}\left(\mathbf{x}_{k|k}^{NL,(i)}\right) \tag{10.a}$$

$$\hat{\mathbf{x}}_{k+1|k}^{L,(i)} \rightarrow \hat{\mathbf{x}}_{k+1|k}^{L,(i)} + L_k\left(\boldsymbol{\xi}_k - A_k^{NL}\hat{\mathbf{x}}_{k|k}^{L,(i)}\right) \tag{10.b}$$

$$P_{k+1|k}^{(i)} \rightarrow P_{k+1|k}^{(i)} - L_k N_k L_k^T \tag{10.c}$$

$$L_k = A_k^{L} P_{k|k}^{(i)} \left(A_k^{NL}\right)^T N_k^{-1} \tag{10.d}$$

$$N_k = A_k^{NL} P_{k|k}^{(i)} \left(A_k^{NL}\right)^T + Q_k^{NL} \tag{10.e}$$

where $a \rightarrow b$ means: "replace the value of a with b". The difference in the linear prediction step of marginalized particle

This article has been accepted for publication in a future issue of this journal, but has not been fully edited. Content may change prior to final publication. Citation information: DOI 10.1109/JBHI.2016.2582340, IEEE Journal of Biomedical and Health Informatics

filter and that of Kalman filter can be understood by inspecting (9.b) and (9.c). Schön *et al.* claimed that in the "triangular model" and "general model" there is hidden information about $\mathbf{x}_k^L$ in $\mathbf{x}_k^{NL}$ and proved that by using the information of predicted nonlinear parts of the particles $(\mathbf{x}_{k+1|k}^{NL,(i)}, i=1,\ldots,N)$, a better prediction of linear parts $(\hat{\mathbf{x}}_{k+1|k}^{L,(i)}, i=1,\ldots,N)$ can be obtained [19].

III. Marginalized Particle EKF for ECG Denoising

In this section, our proposed method for ECG denoising is expressed in detail. First, the modifications in the marginalized particle filter structure are formulated. Then, the method to extract EDM parameters is explained, and finally a novel automatic strategy for particle weighting is expounded.

A. Modification in Marginalized Particle Filter Formulation

To overcome the drawbacks of PF and EKF, a method for denoising ECG using a novel combination of marginalized particle filter and EKF frameworks is proposed here.

We rewrite (2) in the form of:

$$\begin{cases} \mathbf{x}_{k+1}^L = \left(A_k^L \mathbf{x}_k^L + G_k^L \boldsymbol{\omega}_k^L\right) \bmod (2\pi) \\ \mathbf{x}_{k+1}^{NL} = \mathrm{g}\left(\mathbf{x}_k^L, \boldsymbol{\omega}_k^{NL}\right) + f_k^{NL}\left(\mathbf{x}_k^{NL}\right) \end{cases} \tag{11}$$

where $\mathbf{x}_{k+1}^L = \varphi_{k+1}, Q_k^{NL} = E\{\boldsymbol{\omega}_k^{NL}\left(\boldsymbol{\omega}_k^{NL}\right)^{\boldsymbol{T}}\}, G_k^L \boldsymbol{\omega}_k^L = \omega\delta$

$A_k^L = I, \mathbf{x}_{k+1}^{NL} = z_{k+1}, \boldsymbol{\omega}_k^{NL} = \left[\omega, \eta, a_j, b_j, \theta_j\right]^T$. Additionally,

$$g\left(\mathbf{x}_k^L, \boldsymbol{\omega}_k^{NL}\right) = -\sum_{j\in\{P,Q,R,S,T\}} \omega\delta \frac{a_j \Delta\theta_j}{b_j^2} \exp\left(-\frac{\Delta\theta_j^2}{2b_j^2}\right)$$

$\left(j \in P,Q,R,S,T\right)$ and $f_k^{NL}\left(\mathbf{x}_k^{NL}\right) = z_k$. By looking at the 2-state EDM in (11), it is realized that due to the nonlinear term $g\left(\mathbf{x}_k^L, \boldsymbol{\omega}_k^{NL}\right)$, this model is not a "general model", hence it is not a "triangular model" either. In other words, the nonlinear function $g\left(\mathbf{x}_k^L, \boldsymbol{\omega}_k^{NL}\right)$ restricts the implementation of the aforementioned marginalized particle filter algorithm. Furthermore $\boldsymbol{\omega}_k^L \in \boldsymbol{\omega}_k^{NL}$. So, the equations (10.b), (10.d) and (10.e) cannot be used in step 8 of marginalized particle filter algorithm in the current form and some modifications seem to be necessary.

First the 2-state polar EDM should be modified in a way that $\boldsymbol{\omega}_k^L \notin \boldsymbol{\omega}_k^{NL}$. Adding ω (angular velocity) to the state model as an AR state will solve the problem. Of course this approach was previously proposed by Lin *et al.* in [18].With this simple but effective modification, a 3-state polar EDM is constructed:

$$\begin{cases} \varphi_{k+1} = \left(\varphi_k + \omega_k \delta\right) \bmod (2\pi) + \eta_\phi \\ z_{k+1} = -\sum_{j\in\{P,Q,R,S,T\}} \omega_k \delta \frac{a_j \Delta\theta_j}{b_j^2} \exp\left(-\frac{\Delta\theta_j^2}{2b_j^2}\right) + z_k + \eta \\ \omega_{k+1} = \omega_k + \eta_\omega . \end{cases} \tag{12}$$

In this model, $A_k^L\left(\mathbf{x}_k^{NL}\right) = \begin{bmatrix} 1 & \delta \\ 0 & 1 \end{bmatrix}$, $Q_k^{NL} = E\{\boldsymbol{\omega}_k^{NL}\left(\boldsymbol{\omega}_k^{NL}\right)^{\boldsymbol{T}}\}$

$\mathbf{x}_{k+1}^L = [\varphi_{k+1}, \omega_{k+1}]^T$, $\mathbf{x}_{k+1}^{NL} = z_{k+1}, f_k^{NL}\left(\mathbf{x}_k^{NL}\right) = z_k$,

$\boldsymbol{\omega}_k^{NL} = \left[\eta, a_j, b_j, \theta_j\right]^T \left(j \in P,Q,R,S,T\right), \boldsymbol{\omega}_k^L = \left[\eta_\phi, \eta_\omega\right]^T$

, $\mathrm{g}\left(\mathbf{x}_k^L, \boldsymbol{\omega}_k^{NL}\right) = -\sum_{j\in\{P,Q,R,S,T\}} \omega_k \delta \frac{a_j \Delta\theta_j}{b_j^2} \exp\left(-\frac{\Delta\theta_j^2}{2b_j^2}\right)$.

η_ϕ and η_ω are added to the 3-state EDM to model the uncertainties of the linear state equations. In this polar model, the R-peaks are fixed at zero phases. It should be mentioned that although the "mod" operator (in (12)) is not linear, the phase jumps of the mod operator occur during the inter-beat baseline segments of the ECG, which are close to zero and minimally affected by its nonlinear effects. Therefore in practice, φ_{k+1} can be considered as linear state variable.

The only remaining problem is the nonlinear function $g\left(\mathbf{x}_k^L, \boldsymbol{\omega}_k^{NL}\right)$. By considering (11) and (12), first (10.a) is rewritten in the following way:

$$\begin{aligned} \boldsymbol{\xi}_k &= \mathbf{x}_{k+1|k}^{NL,(i)} - f_k^{NL}\left(\mathbf{x}_{k|k}^{NL,(i)}\right) = \mathbf{x}_{k+1|k}^{NL,(i)} - \mathbf{x}_{k|k}^{NL,(i)} \\ &= \mathrm{g}\left(\hat{\mathbf{x}}_{k+1|k}^L, \bar{\boldsymbol{\omega}}_{\boldsymbol{k}}^{\boldsymbol{NL}}\right). \end{aligned} \tag{13}$$

By using EKF concept, $\mathrm{g}\left(\hat{\mathbf{x}}_{k+1|k}^L, \bar{\boldsymbol{\omega}}_{\boldsymbol{k}}^{\boldsymbol{NL}}\right)$ is linearly approximated near a desired reference point $\left(\hat{\mathbf{x}}_{k|k}^L, \bar{\boldsymbol{\omega}}_k^{NL} = \boldsymbol{E}\left\{\boldsymbol{\omega}_k^{NL}\right\}\right)$. The (13) and (4.c) become uncorrelated as well. As a result, the second prediction step expressed in (10) becomes:

$$\boldsymbol{\xi}_k \approx \mathrm{g}\left(\hat{\mathbf{x}}_{k+1|k}^L, \bar{\boldsymbol{\omega}}_{\boldsymbol{k}}^{\boldsymbol{NL}}\right) + \mathcal{A}_k\left(\hat{\mathbf{x}}_{k+1|k}^L - \hat{\mathbf{x}}_{k|k}^L\right) + \mathcal{B}_k\left(\boldsymbol{\omega}_{\boldsymbol{k}}^{\boldsymbol{NL}} - \bar{\boldsymbol{\omega}}_{\boldsymbol{k}}^{\boldsymbol{NL}}\right)$$

$$\mathcal{A}_k = \frac{\partial \mathrm{g}\left(\hat{\mathbf{x}}_{k+1|k}^L, \bar{\boldsymbol{\omega}}_{\boldsymbol{k}}^{\boldsymbol{NL}}\right)}{\partial \hat{\mathbf{x}}_{k+1|k}^L} \Big| \hat{\mathbf{x}}_{k+1|k}^L = \hat{\mathbf{x}}_{k|k}^L \tag{14.a}$$

$$, \mathcal{B}_k = \frac{\partial \mathrm{g}\left(\hat{\mathbf{x}}_{k+1|k}^L, \boldsymbol{\omega}_{\boldsymbol{k}}^{\boldsymbol{NL}}\right)}{\partial \boldsymbol{\omega}_{\boldsymbol{k}}^{\boldsymbol{NL}}} \Big| \boldsymbol{\omega}_{\boldsymbol{k}}^{\boldsymbol{NL}} = \bar{\boldsymbol{\omega}}_{\boldsymbol{k}}^{\boldsymbol{NL}}$$

$$\hat{\mathbf{x}}_{k+1|k}^{L,(i)} \rightarrow \hat{\mathbf{x}}_{k+1|k}^{L,(i)} + L_k\left(\boldsymbol{\xi}_k - \mathrm{g}\left(\hat{\boldsymbol{x}}_{k|k}^L, \bar{\boldsymbol{\omega}}_{\boldsymbol{k}}^{\boldsymbol{NL}}\right)\right) \tag{14.b}$$

$$P_{k+1|k}^{(i)} \rightarrow P_{k+1|k}^{(i)} - L_k N_k L_k^T \tag{14.c}$$

$$L_k = A_k^L\left(\mathbf{x}_k^{NL}\right) P_{k|k}^{(i)} \left(\mathcal{A}_k\right)^T N_k^{-1} \tag{14.d}$$

$$N_k = \mathcal{A}_k P_{k|k}^{(i)} \left(\mathcal{A}_k\right)^T + \mathcal{B}_k Q_k^{NL} \left(\mathcal{B}_k\right)^T . \tag{14.e}$$

This article has been accepted for publication in a future issue of this journal, but has not been fully edited. Content may change prior to final publication. Citation information: DOI 10.1109/JBHI.2016.2582340, IEEE Journal of Biomedical and Health Informatics

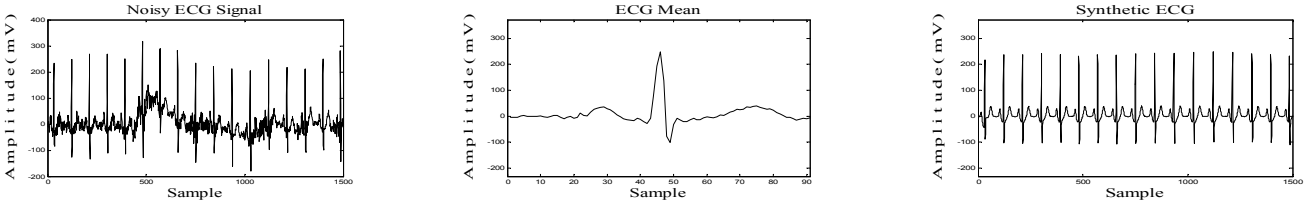

(a) (b) (c)

Fig. 1 Synthetic ECG construction procedure; (a) noisy (MA noise) ECG signal with SNR=3 dB, (b) ECG mean $\overline{ECG}(\theta)$, (c) synthetic ECG ECG_{synth}.

We call this modified algorithm "marginalized particle-extended Kalman filter (MP-EKF) algorithm". It is similar to the 8-step marginalized particle filter explained in section 2, except that in step 8 instead of using (10), (14) is applied.

B. ECG Parameter Extraction and Observation Equations

The parameter extraction procedure in this paper is similar to the approaches in [12]-[15]. First, the R-peaks of ECG cycles in signal are detected and assumed to be positioned at $\theta = 0$. The ECG samples between two sequential R-peaks will have a phase between 0 and 2π (or -π and π). By estimating the mean and variance of each sample in the overlaid ECG cycles, a phase wrapped ECG mean waveform ($\overline{ECG}(\theta)$) and a phase wrapped ECG variance waveform ($\sigma_{ECG}(\theta)$) are built. In [12]-[15], an off-line optimization method based on nonlinear least-squares approach, proposed by Clifford in [21], was used to extract the ECG feature parameters using these two waveforms. The same approach was used here for estimating the optimal values for $\left[a_j, b_j, \theta_j\right]^T$, $j \in \{P, Q, R, S, T\}$. The covariance matrices Q_k^{NL} and Q_k^{L} are constructed by computing the mean and variance of the estimated parameters.

The measurement model is constructed similar to the model proposed in [22]. By detecting the R-peaks and linearly phase assigning to the samples between two consecutive R-peaks, an extra observation is obtained. It is also possible to add a linear observation equation corresponding to the angular velocity. If we differentiate phase in each R-R peak period, an angular velocity observation is obtained. As the phase variation between $-\pi$ and π is considered linear, ω is assumed constant between each R-R peak period but it may be contaminated by noise. As a result, the measurement model is:

$$\begin{bmatrix} \phi_k \\ s_k \\ \Omega_k \end{bmatrix} = \begin{bmatrix} 1 & 0 & 0 \\ 0 & 1 & 0 \\ 0 & 0 & 1 \end{bmatrix} . \begin{bmatrix} \varphi_k \\ z_k \\ \omega_k \end{bmatrix} + \begin{bmatrix} u_k \\ v_k \\ w_k \end{bmatrix} \quad (15)$$

$$, R_k = E\left\{\left[u_k, v_k, w_k\right]^T \left[u_k, v_k, w_k\right]\right\}$$

where $\mathbf{y}_k = \left[\phi_k, s_k, \Omega_k\right]^T$ is the measurement vector and the noise vector $\mathbf{v}_k = \left[u_k, v_k, w_k\right]^T$ describes the measurement model's uncertainty.

C. Particle Weighting

Since the only measurements from ECG signals are the noisy amplitudes, linearly assigned phases, and angular velocities, a particle weighting strategy in each step must be well-defined. If the particle weighting relies only on noisy ECG, the filtered ECG follows the noisy signal which is not desirable. To solve this problem, we propose to use a synthetic ECG signal (ECG_{synth}) which is constructed using the feature parameters extracted from $\overline{ECG}(\theta)$. The length of this synthetic signal is exactly the same as the noisy ECG signal. The location of R-peaks in EC_{synth} overlaps with the location of R-peaks in the noisy ECG signal and the samples between sequential R-peaks are linearly assigned with phases between 0 and 2π. As shown in Fig. 1, $\overline{ECG}(\theta)$ is calculated using phase wrapped ECG cycles. The feature parameters of $\overline{ECG}(\theta)$ are then used to construct ECG_{synth}. The weighting strategy that we propose here, evaluates and weights the particles at each time-step based on their distance to the noisy measurements and ECG_{synth}. We used a statistical distance metric called the "Mahalanobis distance" as the closeness evaluation measure. The weighting strategy in each time-step for each particle $\begin{bmatrix} \hat{\mathbf{x}}_{k|k}^{L,(i)} \\ \mathbf{x}_{k|k}^{NL,(i)} \end{bmatrix}$ is as follows:

1- The Mahalanobis distance between $\begin{bmatrix} \hat{\varphi}_{k|k}^{L,(i)} \\ \hat{z}_{k|k}^{NL,(i)} \\ \hat{\omega}_{k|k}^{L,(i)} \end{bmatrix}$ and $\begin{bmatrix} \phi_k \\ s_k \\ \Omega_k \end{bmatrix}$ is calculated ($\begin{bmatrix} \phi_k \\ s_k \\ \Omega_k \end{bmatrix}$ is measurement vector at time step k) using:

$$d_{measur} = \left[(\hat{\varphi}_{k|k}^{L,(i)} - \phi_k) \left(\hat{z}_{k|k}^{NL,(i)} - s_k \right) \quad (\hat{\omega}_{k|k}^{L,(i)} - \Omega_k) \right]^T \times R_k^{-1} \left[(\hat{\varphi}_{k|k}^{L,(i)} - \phi_k) \left(\hat{z}_{k|k}^{NL,(i)} - s_k \right) \quad (\hat{\omega}_{k|k}^{L,(i)} - \Omega_k) \right]. \quad (16)$$

The value of d_{measur} represents the closeness of the *i*th particle to the current noisy measurement. If this value is small, it suggests that the *i*th particle probably gives a good estimate of states and should get a higher weight, and vice versa. Although weighting the particles using d_{measur} seems quite reasonable in high input SNRs, relying on this value alone in noisy situations doesn't guarantee proper state estimations.

This article has been accepted for publication in a future issue of this journal, but has not been fully edited. Content may change prior to final publication. Citation information: DOI 10.1109/JBHI.2016.2582340, IEEE Journal of Biomedical and Health Informatics

2- The Mahalanobis distance between $\begin{bmatrix} \hat{\varphi}_{k|k}^{L,(i)} \\ \hat{z}_{k|k}^{NL,(i)} \\ \hat{\omega}_{k|k}^{L,(i)} \end{bmatrix}$ and $\begin{bmatrix} \phi_k \\ ecg_{syn}(k) \\ \Omega_k \end{bmatrix}$ is calculated using:

$$d_{synth} = \left[(\hat{\varphi}_{k|k}^{L,(i)} - \phi_k) \left(\hat{z}_{k|k}^{NL,(i)} - ecg_{syn}(k) \right) (\hat{\omega}_{k|k}^{L,(i)} - \Omega_k) \right]^T \times R_k^{-1} [(\hat{\varphi}_{k|k}^{L,(i)} - \phi_k) \left(\hat{z}_{k|k}^{NL,(i)} - ecg_{syn}(k) \right) (\hat{\omega}_{k|k}^{L,(i)} - \Omega_k)]. \quad (17)$$

The value of d_{synth} represents the closeness of the *i*th particle to the current sample in ECG_{synth} ($ecg_{syn}(k)$). If this value is small, it suggests that the *i*th particle probably gives a good estimate of states and should get a higher weight, and vice versa. Because ECG_{synth} has a constant morphology, although particle weighting using d_{synth} alone is a good choice in low input SNRs, the changes in ECG morphology cannot be traced properly, especially in high input SNRs.

3- The weight w_k^i for particle $\begin{bmatrix} \hat{\varphi}_{k|k}^{L,(i)} \\ \hat{z}_{k|k}^{NL,(i)} \\ \hat{\omega}_{k|k}^{L,(i)} \end{bmatrix}$ is calculated:

$$w_k^i = w_{k-1}^i \left(\frac{1}{d_{synth}} + \frac{1}{d_{measur}} \right). \quad (18)$$

With this strategy, the proposed filtering framework relies on both noisy ECG and synthetic ECG signals. This equation automatically involves the behaviors of both noisy and synthetic ECG signals in assigning particle weights. When the ECG signal is too noisy, this weighting scheme automatically enforces the synthetic ECG's characteristics to balance the marginalized particle filter's behavior. However, in a good SNR situation, this scheme forces the filter to not only rely on the synthetic ECG signal but also on the noisy ECG signal.

IV. Results and Discussion

The proposed algorithm was implemented in Matlab on a 12-core computer at 2 GHz with 12 GB RAM capable of parallel processing. To evaluate the performance of our algorithm, the MIT-BIH normal sinus rhythm database from PhysioBank [23] was used. 200 signal segments from different subjects of this database were selected (approximately 20 segments from each record). Each segment was an approximately 30 second signal and contained normal ECG cycles with no significant arrhythmias.

The benchmark methods used in this study were the EKF and EKS algorithms that were firstly introduced in [12] and reported to outperform other techniques (e.g. *Wavelet Transform*) in the field of ECG denoising. Due to the fact that a 3-state polar EDM in the MP-EKF was used, the same modified 3-state model was embedded in the structure of the benchmark methods. Therefore, the proposed method was compared with EKF3 and EKS3. To compare methods properly, we used similar EDM feature parameters and covariance matrices in each simulation.

The denoising performance of the proposed method was investigated in 11 different non-equidistant input SNRs ranging from 10 dB to -5 dB. SNRs 10, 8, 6, 4, 2, 1, 0, -1, -3, -4, -5 dB were chosen because our study was focused on low input SNRs where the model and the measurements are not trustworthy and the performances of the aforementioned filters were challenged veritably. Four different noise types, Gaussian white noise, pink noise, brown noise, and MA noise were chosen. The first three noises were generated according to the following spectral density:

$$S(f) \propto \frac{1}{f^{\beta}} \quad (19)$$

where $S(f)$ and f are the noise spectral density function and frequency in Hz. The parameter β is 0, 1 and 2 for Gaussian white noise, pink and brown noise, respectively. For the non-stationary MA noise simulation, real muscle artifact from the MIT-BIH Noise Stress Test Database was used [24]. This noise was recorded at a sampling rate of 360 Hz and needed to be resampled to 128 Hz (sampling frequency of test signals). For quantitative comparison, the SNR improvement measure was used [13]:

$$\begin{aligned} \mathrm{imp}[\mathrm{dB}] &= \mathrm{SNR}_{\mathrm{output}} - \mathrm{SNR}_{\mathrm{input}} \\ &= 10\log\left(\frac{\sum_i |x_n(i) - x_o(i)|^2}{\sum_i |x_d(i) - x_o(i)|^2} \right) \end{aligned} \quad (20)$$

where x_o, x_n and x_d represent the original ECG signal, the noisy ECG signal and the denoised ECG signal, respectively.

Particle filters and their variants are computationally demanding. Therefore, any performance improvement of PF over traditional Kalman filters should be studied from the cost and benefit viewpoints. In our simulations each test signal received a different random noise input in each SNR. The number of particles for MP-EKF was empirically chosen 200 ensuing 70~80 seconds calculation time for each simulation which was less than 1 second for EKF and EKS. Although our algorithm is much slower (as expected), by looking at Fig. 2, we can see its predominance over EKF/EKS frameworks in non-Gaussian non-stationary situations. Fig. 2 depicts the SNR improvement of the MP-EKF, EKF and EKS frameworks in the presence of Gaussian white noise, pink, brown and MA noise in different input SNRs. From Fig. 2(a) it is realized that the EKS framework achieved best results for input SNRs>1dB in the presence of white Gaussian noise. Also, it can be seen that MP-EKF framework performed better than EKF3 for input SNRs<4dB. The outperformance of EKF3 and EKS3 algorithms over our algorithm in SNRs>4dB in Fig. 2(a) can be justified by realizing the fact that in higher input SNRs, these frameworks could trace signal well for two reasons: 1) the model and the measurements are trustworthy in higher input SNRs, 2) their structures allow them to optimally filter out signals in the

This article has been accepted for publication in a future issue of this journal, but has not been fully edited. Content may change prior to final publication. Citation information: DOI 10.1109/JBHI.2016.2582340, IEEE Journal of Biomedical and Health Informatics

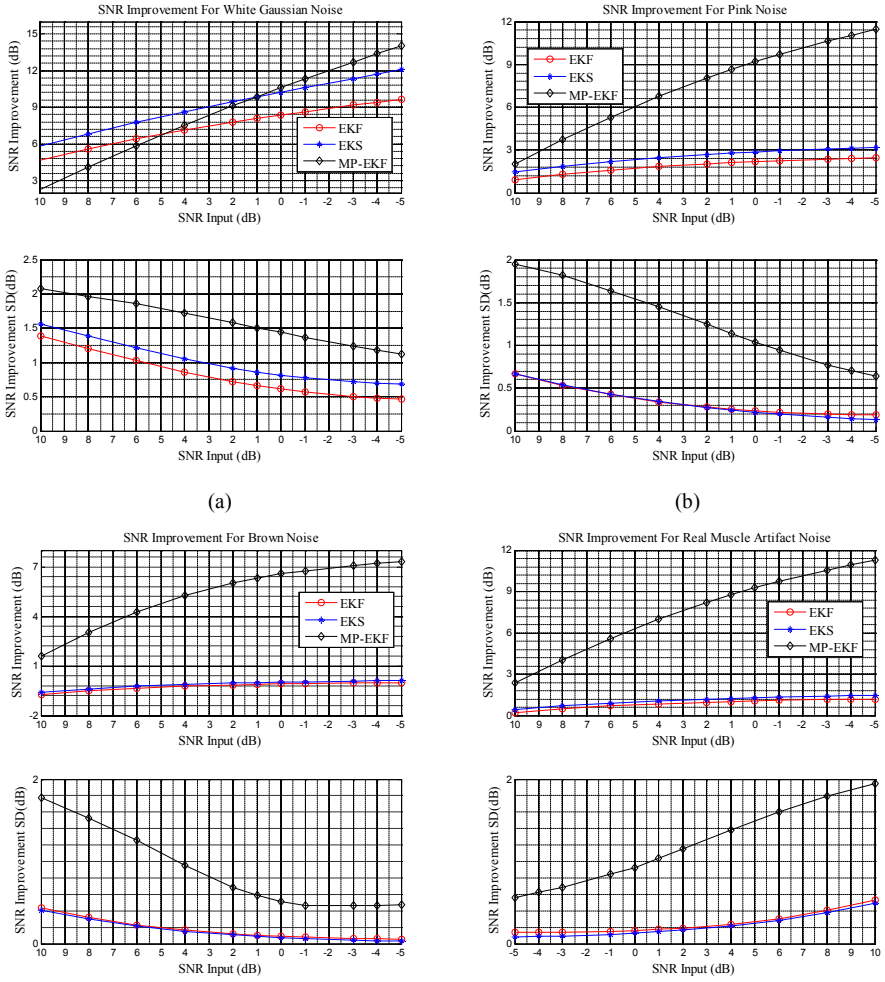

Fig. 2. The mean (top) and standard deviation (bottom) of the filter output SNR improvements versus different input SNRs (a) white Gaussian noise, (b) pink noise, (c) Brown noise, (d) MA noise.

presence of white Gaussian noise. However, the proposed marginalized particle filter apparently needs more particles to reach their accuracy. Nevertheless, the MP-EKF framework outmatches them in lower input SNRs. Figs. 2(b), 2(c) and 2(d) demonstrate the performance comparison of the MP-EKF to the EKF and EKS frameworks in the presence of pink, brown and MA noises in different input SNRs, respectively. With further investigation, it can be realized that the slope of SNR improvement line for EKS and EKF is almost flat in the presence of non-Gaussian noises. It can also be understood that the SNR improvement of EKF and EKS outputs decreases substantially as the additive noise becomes more non-stationary. However, this drop-off in the MP-EKF is the least. For example by looking at Figs. 2(a), 2(b) and 2(c) at input SNR -5 dB, it can be seen that the SNR improvement of MP-EKF decreases from 14.03 dB for white Gaussian noise to 7.3 dB for brown noise. However, the decrement for EKS is from 12.09 dB to 0.10 dB. These figures demonstrate the superiority of the proposed framework over EKF and EKS in non-Gaussian non-stationary situations. An interesting fact can be discovered by looking at Fig. 2(d). It can be noticed that the performance of the MP-EKF in the presence of non-stationary MA noise is much better than its performance in the case of brown noise.

The reason of MP-EKF superiority lies within its nonlinear structure and particle weighting strategy. The assumption of ECG signal as a nonlinear state vector in MP-EKF helps to trace the ECG signals better. Additionally as explained in the previous section, our weighting strategy acts as leverage. When the input SNR is low, the MP-EKF relies on the behavior of synthetic ECG signal too, while in higher input SNRs; it involves the measurements to trace the signal correctly. In addition, this leveraging is done automatically and there is no need to know how noisy the signal is. If the effect of the input noise is known, we can desirably adjust (18). For example if it is known that the input noise has a high power spectrum, by using (21), we can reduce the effect of noisy measurements by reducing the coefficient of d_{measur} and instead increase the coefficient of d_{synth} $(\alpha_1 > \alpha_2)$ to impose the behavior of synthetic ECG on the particles:

This article has been accepted for publication in a future issue of this journal, but has not been fully edited. Content may change prior to final publication. Citation information: DOI 10.1109/JBHI.2016.2582340, IEEE Journal of Biomedical and Health Informatics

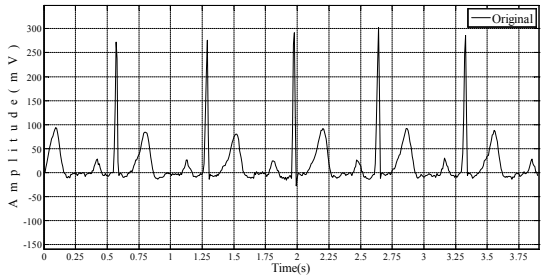

(a)

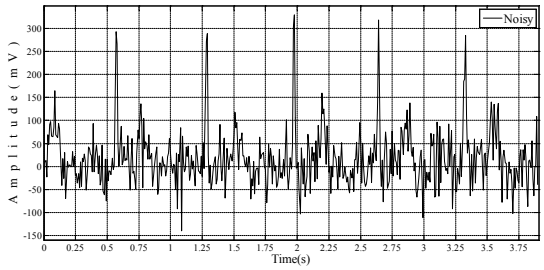

(b)

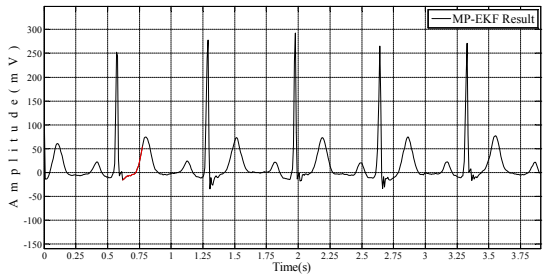

(c)

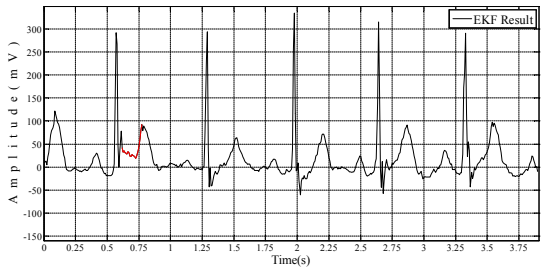

(d)

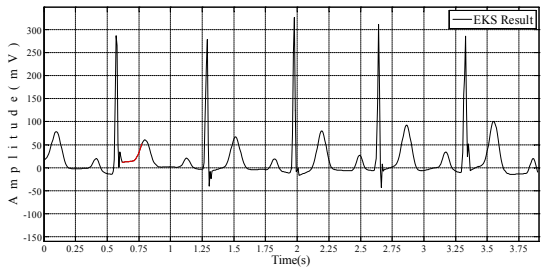

(e)

Fig. 3. Typical filtering results for record "19140" in the presence of white Gaussian noise in SNR 2 dB. (a) Original, (b) Noisy, (c) MP-EKF, (d) EKF, (e) EKS.

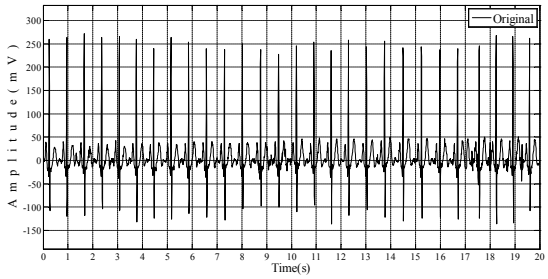

(a)

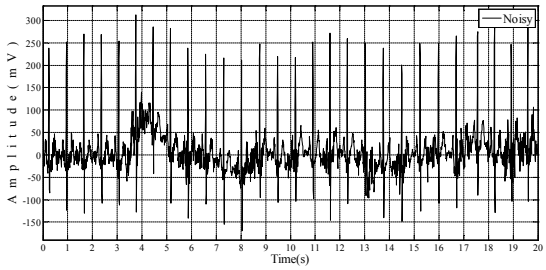

(b)

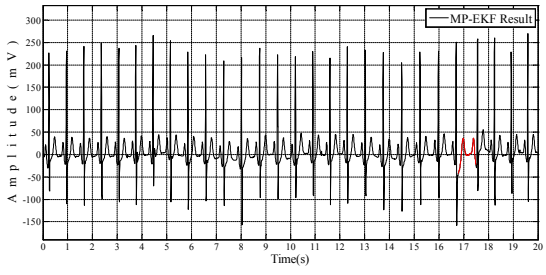

(c)

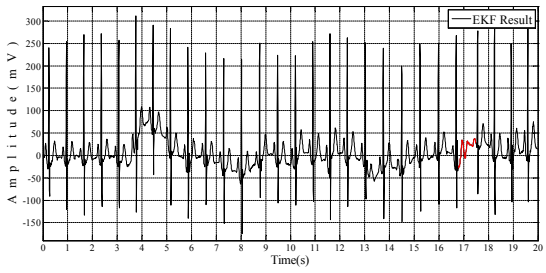

(d)

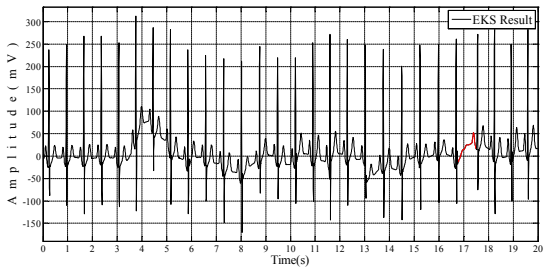

(e)

Fig. 4. Typical filtering results for record "19090" in the presence of MA noise in SNR 6dB. (a) Original, (b) Noisy, (c) MP-EKF, (d) EKF, (e) EKS.

$$w_k^i = w_{k-1}^i \left(\frac{\alpha_1}{d_{synth}} + \frac{\alpha_2}{d_{measur}} \right) \tag{21}$$

The aforementioned characteristics of MP-EKF exhibit their grandness in the presence of non-Gaussian and non-stationary noises. Fig. 3 represents an example of denoising in the presence of Gaussian noise at input SNR of 2 dB for an ECG episode of record "19140". From Fig. 3, it can be seen that all methods have effectively denoised the distorted ECG signal. It is obvious

This article has been accepted for publication in a future issue of this journal, but has not been fully edited. Content may change prior to final publication. Citation information: DOI 10.1109/JBHI.2016.2582340, IEEE Journal of Biomedical and Health Informatics

Table I. Performance evaluation of MP-EKF, EKF, and EKS frameworks in the presence of white Gaussian and pink noises from MSEPWRD viewpoint.

	MSEPWRD ($mean \pm SD$) (mV)							
	Gaussian White Noise				Pink Noise			
METHOD	0 dB	-1 dB	-3 dB	-5dB	0 dB	-1 dB	-3 dB	-5dB
MP_EKF	1.284±0.225	1.329±0.224	1.434±0.231	1.552±0.242	1.322±0.204	1.387±0.202	1.550±0.209	1.755±0.228
EKS	1.358±0.180	1.458±0.196	1.678±0.237	1.923±0.288	2.192±0.288	2.415±0.325	2.939±0.414	3.585±0.528
EKF	1.677±0.183	1.824±0.200	2.158±0.242	2.552±0.297	2.395±0.310	2.65±0.351	3.251±0.451	3.994±0.576

Table II. Performance evaluation of MP-EKF, EKF, and EKS frameworks in the presence of brown noise and real muscle artifact from MSEPWRD viewpoint.

	MSEPWRD ($mean \pm SD$) (mV)							
	Brown Noise				Real Muscle Artifact			
METHOD	0 dB	-1 dB	-3 dB	-5dB	0 dB	-1 dB	-3 dB	-5dB
MP_EKF	1.335±0.204	1.408±0.205	1.585±0.219	1.810±0.251	1.468±0.199	1.552±0.200	1.747±0.223	1.987±0.255
EKS	2.231±0.299	2.460±0.337	3.001±0.431	3.672±0.552	2.933±0.455	3.247±0.514	3.992±0.656	4.918±0.836
EKF	2.399±0.315	2.655±0.356	3.261±0.457	4.013±0.584	3.057±0.473	3.393±0.534	4.188±0.681	5.179±0.866

that the proposed filter has outperformed the EKF method. However because of back tracking algorithm utilized by EKS, its output provides the smoothest but not best result. By comparing filtered outputs carefully at Fig. 3 around time 0.6-0.75 sec (marked by red color), a baseline elevation can be noticed from EKF output that disfigures the ECG's natural morphology. Although this elevation is reduced in EKS output, it's still noticeable. This is because EKS uses only EKF estimates and if it is not provided with good estimates it cannot contribute a good result. For further illustration, an example of denoising in the presence of MA noise at input SNR of 6 dB for record "19090" is demonstrated in Fig. 4. In this figure, in addition to change in the R-peaks amplitudes, in some ECG cycles, the T-wave and P-wave segments are corrupted. It is shown in this figure that the EKF and EKS outputs have baseline drifts which are reduced significantly in the MP-EKF due to its weighting strategy. In baseline drift situation, this strategy automatically stabilizes the particles' behaviors by involving the characteristics of synthetic ECG (which has no baseline drifts), consequently reducing the baseline drift. In addition, the R-peak amplitudes in MP-EKF are nearer to their original amplitudes in comparison to the EKF and EKS outputs. Furthermore, around time interval 17-17.5 sec (marked by red color), the P-wave and T-wave segments are completely removed in the EKF and EKS outputs, respectively, while both are successfully recovered using MP-EKF owing to its nonlinear structure.

Because ECG is a clinically important physiological signal and the morphology of this signal contains vital information about cardiac activity, a very significant aspect of ECG signal processing method is make sure that the diagnostic signal information is well-preserved after filtering. Use of SNR improvement as a quantitative measure does not guarantee that the proposed filtering method outperforms EKF/EKS frameworks in preserving the diagnostic signal information. Therefore, we evaluated the performances of these frameworks in terms of an ECG diagnostic distortion measure called the "Multi-Scale Entropy Based Weighted Distortion Measure" or MSEWPRD [25]. This metric is a weighted percentage root-mean-square difference (WPRD) between the sub-band wavelet coefficients of the original and filtered signals with weights equal to the multi-scale entropies of the corresponding sub-bands. With this measure, a correct representation of filtered signal distortion at all sub-bands can be achieved [25]. To calculate this metric, both signals must be decomposed using wavelet filters up to L levels. The number of levels depends on the nature of the signal and the sampling frequency. In ECG, in addition to sharp segments (QRS complexes), there are slow waves like P and T waves. A good ECG decomposition includes decent representation of QRS complexes in detail coefficients and P&T waves in approximation coefficients. Therefore, we implemented Daubechies 9/7 bi-orthogonal wavelet filters [26] for ECG decomposition and found L = 4 to be a good choice for sampling frequency of 128 Hz [27].

Tables I and II represent the MP-EKF and EKF/EKS performance evaluations (from MSEWPRD viewpoint) for 4 different noise types and at 4 different input SNRs. We chose low input SNRs: 0, -1, -3, -5 dB to investigate the aforementioned diagnostic distortion metric in the case of highly noise contaminated ECG signals. The results in Tables I and II were calculated by computing the MSEWPRDs of 200 filtered ECG segments chosen from MIT-BIH normal sinus rhythm database. By looking at these results, we can see that the MSEPWRD for each method is higher in lower input SNRs. In addition, as the additive noise becomes more non-stationary, this metric increases significantly for EKF/EKS frameworks but with much lower rate for MP-EKF. For example, by moving from white Gaussian noise toward muscle artifact, the mean MSEWPRD at SNR of -5 dB increases from 2.158 to 5.179 for EKF framework. However, this increment is from 1.552 to 1.987 for the proposed MP-EKF. It is also noticeable that although the EKS structure outperformed the EKF framework, our proposed algorithm had the lowest MSEPWRD in all noise types and at all selected input SNRs. This indicates that the MP-EKF preserves the morphology and diagnostic information of the ECG signals much better than EKF/EKS frameworks, especially in non-Gaussian non-stationary situations.

This article has been accepted for publication in a future issue of this journal, but has not been fully edited. Content may change prior to final publication. Citation information: DOI 10.1109/JBHI.2016.2582340, IEEE Journal of Biomedical and Health Informatics

V. Conclusion

The EKF/EKS frameworks consider EDM as a nonlinear state space model and try to recursively estimate the states by linearizing the EDM. This approach has shortcomings in denoising ECG signals in low input SNRs and in non-Gaussian and non-stationary situations. To resolve this problem, in this paper a nonlinear Bayesian filtering framework is presented. Unlike EKF or particle filter, our framework treats EDM as a mixed linear/nonlinear state space model and uses the properties of both particle filter and extended Kalman filter to efficiently approximate the posterior density of ECG and the linear states. Moreover, the proposed scheme has less computational complexity (in comparison to particle filter approach) and attains better estimations of the linear states in EDM. The experiments showed that in the presence of Gaussian white noise, our proposed framework outperforms the EKF and EKS algorithms in lower input SNRs. They also indicated that it exhibits better results in non-Gaussian non-stationary situations such as presence of pink noise, brown noise and real muscle artifacts in all input SNRs. In addition, the impact of the proposed filtering method on the distortion of diagnostic features of the ECG was investigated and compared with EKF/EKS methods for 4 different noise types at 4 low input SNRs using MSEWPRD metric. The results revealed that our proposed algorithm has the lowest MSEPWRD in all noise types and at low input SNRs and it can conserve the morphology and diagnostic information of the ECG signals much better than EKF/EKS frameworks, especially in non-Gaussian non-stationary situations.

References

[1] G. B. Moody and R. G. Mark, "QRS morphology representation and noise estimation using the Karhunen-Loeve transform," in *Proc. Computers in Cardiology*, 1989, pp. 269-272.

[2] A. K. Barros, A. Mansour, and N. Ohnishi, "Removing artifacts from electrocardiographic signals using independent components analysis," *Neurocomputing,* vol. 22, no. 1, pp. 173-186, 1998.

[3] T. He, G. Clifford, and L. Tarassenko, "Application of independent component analysis in removing artefacts from the electrocardiogram," *Neural Computing & Applications,* vol. 15, no. 2, pp. 105-116, 2006.

[4] G. Clifford, L. Tarassenko, and N. Townsend, "One-pass training of optimal architecture auto-associative neural network for detecting ectopic beats," *Electronics letters,* vol. 37, no. 18, pp. 1126-1127, 2001.

[5] H. Kestler, M. Haschka, W. Kratz, F. Schwenker, G. Palm, V. Hombach, *et al.*, "De-noising of high-resolution ECG signals by combining the discrete wavelet transform with the Wiener filter," in *Proc. Computers in Cardiology* 1998, pp. 233-236.

[6] M. Popescu, P. Cristea, and A. Bezerianos, "High resolution ECG filtering using adaptive Bayesian wavelet shrinkage," in *Proc. Computers in Cardiology*, 1998, pp. 401-404.

[7] P. Agante and J. M. De Sá, "ECG noise filtering using wavelets with soft-thresholding methods," in *Proc. Computers in Cardiology*, 1999, pp. 535-538.

[8] P. Lander and E. J. Berbari, "Time-frequency plane Wiener filtering of the high-resolution ECG: development and application," *IEEE Trans. Biomedical Engineering,* vol. 44, no. 4, pp. 256-265, 1997.

[9] N. V. Thakor and Y.-S. Zhu, "Applications of adaptive filtering to ECG analysis: noise cancellation and arrhythmia detection," *IEEE Trans. Biomedical Engineering,* vol. 38, no. 8, pp. 785-794, 1991.

[10] P. Laguna, R. Jane, O. Meste, P. W. Poon, P. Caminal, H. Rix, *et al.*, "Adaptive filter for event-related bioelectric signals using an impulse correlated reference input: comparison with signal averaging techniques," *IEEE Tran. Biomedical Engineering,* vol. 39, no. 10, pp. 1032-1044, 1992.

[11] P. E. McSharry, G. D. Clifford, L. Tarassenko, and L. A. Smith, "A dynamical model for generating synthetic electrocardiogram signals," *IEEE Trans. Biomedical Engineering,* vol. 50, no. 3, pp. 289-294, 2003.

[12] R. Sameni, M. B. Shamsollahi, C. Jutten, and G. D. Clifford, "A nonlinear Bayesian filtering framework for ECG denoising," *IEEE Trans. Biomedical Engineering,* vol. 54, no. 12, pp. 2172-2185, 2007.

[13] O. Sayadi and M. B. Shamsollahi, "ECG denoising and compression using a modified extended Kalman filter structure," *IEEE Trans. Biomedical Engineering,* vol. 55, no. 9, pp. 2240-2248, 2008.

[14] O. Sayadi and M. Shamsollahi, "A model-based Bayesian framework for ECG beat segmentation," *Physiological Measurement,* vol. 30, no. 3, p. 335, 2009.

[15] O. Sayadi, M. B. Shamsollahi, and G. D. Clifford, "Robust detection of premature ventricular contractions using a wave-based bayesian framework," *IEEE Trans. Biomedical Engineering,* vol. 57, no. 2, pp. 353-362, 2010.

[16] M. S. Arulampalam, S. Maskell, N. Gordon, and T. Clapp, "A tutorial on particle filters for online nonlinear/non-Gaussian Bayesian tracking," *IEEE Trans. Signal Processing,* vol. 50, no. 2, pp. 174-188, 2002.

[17] J. Lee, D. D. McManus, P. Bourrell, L. Sörnmo, and K. H. Chon, "Atrial flutter and atrial tachycardia detection using Bayesian approach with high resolution time–frequency spectrum from ECG recordings," *Biomedical Signal Processing and Control,* vol. 8, no. 6, pp. 992-999, 2013.

[18] C. Lin, M. Bugallo, C. Mailhes, and J.-Y. Tourneret, "ECG denoising using a dynamical model and a marginalized particle filter," in *Proc. ASILOMAR*, 2011, pp. 1679-1683.

[19] T. Schon, F. Gustafsson, and P.-J. Nordlund, "Marginalized particle filters for mixed linear/nonlinear state-space models," *IEEE Trans. Signal Processing,* vol. 53, no. 7, pp. 2279-2289, 2005.

[20] A. Doucet, N. J. Gordon, and V. Krishnamurthy, "Particle filters for state estimation of jump Markov linear systems," *IEEE Trans. Signal Processing,* vol. 49, no. 3, pp. 613-624, 2001.

[21] G. Clifford, A. Shoeb, P. McSharry, and B. Janz, "Model-based filtering, compression and classification of the ECG," *International Journal of Bioelectromagnetism,* vol. 7, no. 1, pp. 158-161, 2005.

[22] M. Akhbari, M. B. Shamsollahi, C. Jutten, and B. Coppa, "ECG denoising using angular velocity as a state and an observation in an extended kalman filter framework," in *Proc. EMBC*, 2012, pp. 2897-2900.

[23] C. The MIT-BIH Normal Sinus Rhythm Database.PhysioNet, MA. [Online]. Available: http://www.physionet.org/physiobank/database/nstdb/

[24] C. The MT-BIH Noise Stress Test Database. PhysioNet, MA. [Online]. Available: http://www.physionet.org/physiobank/database/nstdb/

[25] M. S. Manikandan and S. Dandapat, "Multiscale entropy-based weighted distortion measure for ECG coding," *IEEE Signal Processing Letters,* vol. 15, pp. 829-832, 2008.

[26] M. Antonini, M. Barlaud, P. Mathieu, and I. Daubechies, "Image coding using wavelet transform," *IEEE Trans. Image Processing,* vol. 1, no. 2, pp. 205-220, 1992.

[27] M. S. Manikandan and S. Dandapat, "Wavelet energy based diagnostic distortion measure for ECG," *Biomedical Signal Processing and Control,* vol. 2, no. 2, pp. 80-96, 2007.